Disorder stabilized breached-pair phase in an *s*-wave superconductor

Madhuparna Karmakar,[1,2,*] Subhojit Roy,[1,†] Shantanu Mukherjee,[1,‡] and Rajesh Narayanan[1,§]
[1]*Department of Physics, Indian Institute of Technology Madras, Chennai 600036, India*
[2]*Centre for Quantum Science and Technology, Chennai Institute of Technology, Chennai - 600037, India*

(Received 21 March 2022; revised 4 August 2022; accepted 26 September 2022; published 5 December 2022)

The breached-pair state wherein superconductivity coexists with magnetic polarization is known to exist as a ground state of an imbalanced Fermi system only under very fine-tuned conditions. Here, we show that an *s*-wave superconductor that is well described by a spin-selectively disordered attractive Hubbard model away from half filling has the breached-pair state as a ground-state without the need for such fine-tuning. The existence of this breached-pair phase is established by laying recourse to a Monte Carlo technique called static path approximation (SPA). Further, by using the SPA, we map out the entire phase diagram of the spin-selectively disordered attractive Hubbard model and show that apart from the breached-pair phase, the many-body system hosts the putative *s*-wave superconducting state and a polarized Fermi-liquid state.

DOI: 10.1103/PhysRevResearch.4.043159

I. INTRODUCTION

Recently, there has been a resurgence of interest in realizing ground states wherein superconducting (SC) order coexists with magnetic order. These investigations are not just centered around conventional solid-state systems [1–3] but also include systems that lie in the field of ultracold atomic gases [4–6]. One such possible coexistent phase, namely, Fulde-Ferrell-Larkin-Ovchinnikov (FFLO) [7,8] (which is a SC phase with a finite-q modulation), has now been both theoretically [9–16] and experimentally [1–6] well explored. This of course raises the interesting question of whether it is possible to obtain a stable ground state wherein a homogeneous ($q = 0$) SC order coexists with magnetism in an *s*-wave superconductor. Sarma in a seminal work [17] showed the possible existence of such a homogeneous state with two gapless Fermi surfaces in an *s*-wave superconductor in the presence of an external magnetic field. Called the Sarma phase or the breached pair (BP) phase, this state is shown to arise at the maximum of the thermodynamic potential and thus cannot be a stable ground state.

Driven by advances in cold atomic gas systems, the search for ground states that display unconventional order akin to the BP phase or the FFLO phase received a renewed impetus. For instance, it was conjectured that such a BP phase could exist as a ground state in imbalanced Fermi systems with an attractive on-site interaction [18]. The BP phase was also shown to arise in the context of a lattice fermion model for spin-imbalanced *s*-wave superconductors within a mean-field type description [10]. However, the BP phase of Ref. [18] dubbed as the Liu-Wilczek-Sarma phase was shown to be unstable to a phase-separated state comprising puddles of polarized fluid in the otherwise uniform superfluid state [19]. Furthermore, it was later established via nonperturbative theories [15] and experiments on ultracold atomic gases [5] that for imbalanced superconductors with *s*-wave pairing [10], the BP constitutes a finite temperature phase and is unstable against a homogeneous, gapped SC phase at the ground state.

It was, however, soon realized that the Liu-Wilczek-Sarma phase could be stabilized via fine-tuning the Hamiltonian to include momentum-dependent interactions [20,21]. In the context of momentum-dependent interactions, a recent study has shown that the BP phase can be stabilized as a ground state in unconventional superconductors with $d_{x^2-y^2}$ pairing [22]. The nodes in the SC gap of a d-wave superconductor serve as a host to the unpaired fermions, thereby giving rise to a finite magnetic polarization which coexists with the superconducting order. Further, in the context of cold atomic systems, it was suggested that a variant of the Liu-Wilczek-Sarma phase with just one gapless Fermi surface could be stabilized as the ground state in a two-component Fermi mixture deep in the BEC side of a BCS-BEC crossover [20]. So far, no experimental realization of this quantum BP phase (i.e., BP phase at the ground state) has been reported, which motivates one to come up with a suitable experimental protocol to realize the same. In principle, a Pauli-limited unconventional superconductor such as $CeCoIn_5$, κ-BEDT, etc. [1–3,23,24] when subjected to a moderate in-plane Zeeman field should be able to stabilize a quantum BP phase, but the same has not been reported so far. On the other hand, realizing a momentum-dependent pairing state in an ultracold atomic gas setup is nontrivial.

In this paper, we present an alternate and, arguably, a simpler route to stabilize a quantum BP phase in an

*madhuparna.k@gmail.com
†sjr@physics.iitm.ac.in
‡shantanu@iitm.ac.in
§rnarayanan@iitm.ac.in

s-wave superconductor. This route entails the introduction of a spin-selective disorder potential wherein the two species of fermions see different disorder potentials. Experimentally, such spin-dependent potentials can be realized in optical lattices with randomness being introduced as speckle disorder [25–29]. In other words, experimental realization of such spin-selective disorder can be thought of as a natural extension of combining spin-dependent potential (which have been proposed and experimentally realized) with disorder induced on site randomness. A possible route to introduce randomness in such cold atomic systems is via a speckle-type disorder which is obtained by focusing the light beam that is generated by scattering off a diffusive plate onto the optical lattice that is formed by the interference of counterpropagating lasers.

Additionally, polarized two-dimensional (2D) superconductors emerging at the interface of oxide heterostructures (for example, $LaAlO_3/SrTiO_3$ heterostructure), when subjected to a random quenched disorder, can serve as an ideal platform to realize the quantum BP phase [30–33].

Our starting point is the 2D attractive Hubbard model on a square lattice, with spin-selective random potential disorder $V_{i\sigma}$ at each site:

$$H = -t \sum_{\langle ij\rangle,\sigma} (c^{\dagger}_{i\sigma} c_{j\sigma} + c^{\dagger}_{j\sigma} c_{i\sigma}) - |U| \sum_{i} \hat{n}_{i\uparrow}\hat{n}_{i\downarrow} + \sum_{i\sigma} (V_{i\sigma} - \mu)\hat{n}_{i\sigma}. \quad (1)$$

Here, in Eq. (1), the $c_{i\sigma}$ ($c^{\dagger}_{i\sigma}$) are the fermion annihilation (creation) operators at site i for the fermion species, $\sigma = \uparrow, \downarrow$. In what follows, all energy scales in the model are normalized with respect to the nearest-neighbor hopping amplitude t, which we set to one. The density of the fermions (filling) is dictated by the global chemical potential μ. The disorder potential $V_{i\sigma}$ is set to be spin selective, such that $V_{i\uparrow}=0$ and $V_{i\downarrow} \neq 0$, selected randomly from a box distribution of $[-V/2,V/2]$. The on-site interaction is incorporated through the attractive $|U| > 0$ Hubbard term.

To avoid issues stemming from the well-known degeneracy between the charge density wave and SC orders at $T = 0$ in the clean limit ($V = 0$) of this model for the case of the half-filled lattice ($\langle n\rangle = 1$) [34,35], we work in the regime where the total density is fixed to $\langle n\rangle = 0.85$.

The version of the Hamiltonian in Eq. (1) with spin-independent disorder ($V_{\uparrow} = V_{\downarrow} \neq 0$) has been well studied [36–41]. These studies show a disorder driven superconductor-insulator transition, such that beyond a critical disorder $V > V_c$, the energy states are localized.

The phase diagram of the spin-selective disordered attractive Hubbard model has been investigated within the framework of Bogoliubov–de Gennes mean-field theory (BdG-MFT) [27,42,43]. These studies suggest the existence of two critical disorder strengths V_{c1} and V_{c2}, such that the system is a gapped superconductor for $V < V_{c1}$ and an insulator for $V > V_{c2}$; in the regime $V_{c1} < V < V_{c2}$, a gapless SC state is realized.

In this paper, by using a nonperturbative numerical scheme viz. Static path approximation (SPA) [15,37,44], we study the Hamiltonian shown in Eq. (1). Our key results for the spin-selectively disordered attractive Hubbard model are encoded in the schematic phase diagram shown in Fig. 1. In particular, it shows the existence of a BP phase in addition to the usual fully gapped superconductor and a polarized Fermi liquid. For a constant value of the Hubbard interaction $|U|$, it shows that the BP phase is stabilized for an intermediate range of disorder strengths $V_{c1} < V < V_{c2}$. Furthermore, Fig. 1 also shows that at a constant value of disorder V, the system undergoes a transition from a polarized Fermi liquid to a BP phase and further into a fully gapped superconductor as function of increasing U. A variety of thermodynamic and quasiparticle indicators are used to characterize the BP ground state, and other competing ground states inherent in the system using the SPA method. As we shall soon see (Sec. II), the SPA method retains spatial fluctuations at all length scales, implying that it is sensitive to effects (especially in low dimensions) that cannot be captured by a mean-field approach to the problem.

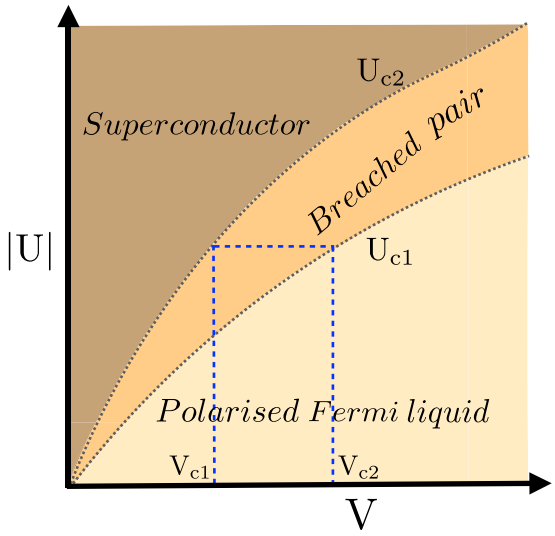

FIG. 1. A schematic phase diagram that describes the various phases hosted by the spin-selectively disordered attractive Hubbard model as a function of the disorder strength. At a constant interaction strength U, with increasing disorder strength V, the spin-selectively disordered model goes from a BCS type ground state with a finite hard gap and zero magnetic polarization to a BP phase. The BP phase is a gapless superconducting ground state with a finite magnetic polarization. With a further increase in V, the system goes over into a polarized Fermi liquid.

The paper is organized as follows: Section II is dedicated to a brief elucidation of the SPA method and the observables that we employ to characterize the spin-selectively disordered attractive Hubbard model. Section III concerns itself with the exposition of the key results of this paper. In particular, Sec. III A is dedicated to the study of the model as a function of disorder while the interaction is kept fixed to a constant value. In a similar fashion, Sec. III B concerns itself with the exploration of the system as a function of the interaction strength while keeping the disorder strength fixed to a constant value. The discussions and conclusions based on our analysis of Sec. III are given in Sec. IV. Finally, in Appendix 1, we elucidate in detail the formalism involved in the SPA scheme and also compare and contrast this method with other techniques that are in vogue in the study of strongly correlated

systems. The details of the Monte Carlo (MC) scheme are fully described in Appendix 2. Finally, in Appendix 3, the results of the BdG-type analysis of the spin-selectively disordered superconductor is placed in comparison with the results that are obtained via a SPA analysis.

II. METHOD AND OBSERVABLE

We decompose the quartic interaction term in Eq. (1) into pairing and density channels by using the Hubbard-Stratonovich (HS) transformation (see Appendix 1). This involves introducing the corresponding bosonic auxiliary fields $\Delta_i(\tau)$ and $\phi_i(\tau)$, respectively. The auxiliary fields are treated classically (by retaining only the $\Omega_n = 0$ Matsubara mode), within the purview of SPA [15,37,44]. The resulting effective Hamiltonian reads

$$\begin{aligned} H_{\text{eff}} = &- \sum_{\langle ij\rangle,\sigma} t_{ij}(c^{\dagger}_{i\sigma}c_{j\sigma} + \text{H.c.}) - \sum_{i}(\Delta_i c^{\dagger}_{i\uparrow}c^{\dagger}_{i\downarrow} + \Delta^{*}_i c_{i\downarrow}c_{i\uparrow}) \\ &- \sum_{i,\sigma}\phi_i c^{\dagger}_{i\sigma}c_{i\sigma} + \sum_{i,\sigma}(V_{i\sigma} - \mu)c^{\dagger}_{i\sigma}c_{i\sigma} \\ &+ \sum_{i}\big(\mid\Delta_i\mid^2 + \phi_i^2\big)/\mid U\mid . \end{aligned} \tag{2}$$

The pairing and density field configurations are controlled by the Boltzmann weight, $P\{\Delta_i, \phi_i\} \propto \text{Tr}_{c^{\dagger},c}e^{-\beta S_{\text{eff}}}$, where S_{eff} is the effective action. For large and random configurations, the trace is taken numerically. The required configurations $\{\Delta_i, \phi_i\}$ are generated by the MC technique, wherein H_{eff} (the effective Hamiltonian) is diagonalized for each attempted update. The optimized configurations $\{\Delta_i, \phi_i\}$ are then used to compute the various correlation functions and quasiparticle indicators that we elucidate below. The observables discussed in this paper are averaged over ten disorder realizations and over 200 MC configurations, (Appendix 2 gives the complete details of the MC scheme we adopt). We characterize the system based on the indicators:

(i) The disorder averaged SC phase stiffness, ρ_s.

(ii) The magnetic polarization of a particular disorder realization, $m_i = \frac{n_{i\uparrow}-n_{i\downarrow}}{n_{i\uparrow}+n_{i\downarrow}}$, and its disorder averaged counterpart m.

(iii) The disorder-averaged spin-resolved single-particle density of states (DOS), $N_{\uparrow}(\omega) = (1/N)\sum_i \mid u^i_n \mid^2 \delta(\omega - E_n)$ and $N_{\downarrow}(\omega) = (1/N)\sum_i \mid v^i_n \mid^2 \delta(\omega + E_n)$.
Here, u^i_n and v^i_n are the eigenvectors corresponding to the eigenvalues E_n.

To determine the SC phase stiffness, we have applied a phase twist to the system through a complex hopping parameter $t \rightarrow te^{i\int \mathbf{A}.dl}$, where $\mathbf{A}$ is the vector potential [45]. The difference between the resulting free-energy density of the system and the free energy corresponding to the untwisted system gives the measure of the SC phase stiffness. The results presented in this paper correspond to a system size of $L = 32$, unless specified otherwise. However, we have checked for finite-size effects and have found our results to be robust against the system-size variation.

At this juncture, it is important to contrast our approach to that developed in Refs. [42,43] for a similar problem. More specifically, in Refs. [42,43] the authors worked with a spin-dependent chemical potential μ_{σ}, which aids in fixing the number density of the individual fermionic species. Thus, as a consequence there are two separate equations for the number density which has to be solved self-consistently (along with the gap equation) to obtain the ground states. These two separate equations for the number density of individual spin species necessitates the introduction of two spin-dependent HS fields ($\phi_{i\sigma}$). Here, in contrast, we fix the total number density of fermions in the system. This thus implies that there is a spin-independent chemical potential μ, which fixes the total number density of the fermions in the model. Thus, we employ a single HS field ϕ_i that couples to both the spin species.

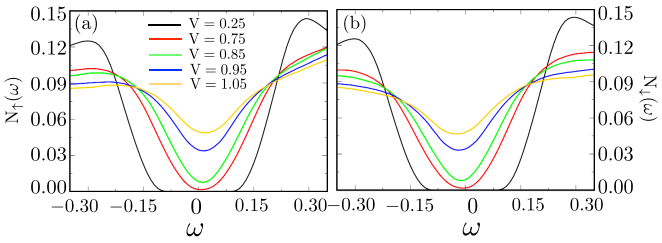

FIG. 2. Disorder dependence of the spin-resolved single particle DOS for the (a) up $[N_{\uparrow}(\omega)]$ and the (b) down $[N_{\downarrow}(\omega)]$ spin species, at the selected interaction of $|U| = 2$. Increasing disorder leads to progressive accumulation of the spectral weight at the Fermi level, thereby leading to the crossover from gapped to gapless superconducting states. A finite spectral weight at the Fermi level is associated with the broadening of the phase coherence peaks via transfer of spectral weight away from the Fermi level.

III. RESULTS

In this section, we analyze the spin-selectively disordered superconductor in terms of its thermodynamic and spectroscopic signatures. All our results are obtained at $T = 0.01t$, which we consider to be concomitant with the ground state. Further lowering of the temperature does not affect the results that are presented in this paper.

A. The phase diagram as a function of disorder

Here, we study the phase diagram of the model for a fixed value of $|U| = 2$ as a function of the disorder strength V. In particular, we first focus on the results depicted in Figs. 2 and 3. Specifically, Figs. 2(a), and 2(b) show the behavior of the DOS corresponding to the up- and down-spin species, respectively, as a function of the disorder strength at a fixed value of $|U| = 2$. As can be clearly seen, with increasing disorder, the gap vanishes for both up- and down-spin species. This behavior for the DOS (at weaker interaction strengths) can be modeled by means of a variation of the Abrikosov-Gorkov (AG)-type formalism [43,46] for paramagnetic impurities in disordered s-wave superconductors. However, in this adaptation of the AG theory, one needs to account for two different pair-breaking times ($\tau_{\uparrow}$, and $\tau_{\downarrow}$ for the up- and down-spin species, respectively) reflective of the spin-selectivity of the disorder potential. Furthermore, our implementation of the disorder would imply that at the bare level, $\tau_{\uparrow}$ is infinite, which gets rendered to a large (with $\tau_{\uparrow} \gg \tau_{\downarrow}$) but finite value via renormalization effects due to a finite U (the disorder is

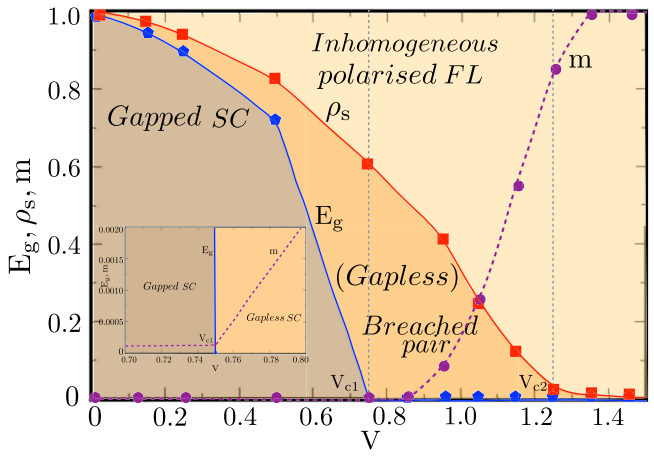

FIG. 3. Ground-state phase diagram of superconductor in presence of spin-selective potential disorder at a filling of $n = 0.85$. The different curves correspond to (i) single-particle energy gap at the Fermi level (E_g), (ii) superconducting phase stiffness (ρ_s), and (iii) average magnetic polarization (m), plotted as a function of disorder strength; the dashed line corresponds to the fitting (see text). The scales are normalized appropriately. The inset is a zoom-in near the V_{c1}, which attests to the fact that the magnetic polarization picks up when E_g goes to zero.

transferred to the up spin via interaction effects). Thus, within this caveat of two different phenomenological pair-breaking times, the DOS for both the up and down species conforms exactly to the results of the AG theory [46].

Now, the results presented in Fig. 2 are used to map out, with respect to disorder, the behavior of the single-particle energy gap at the Fermi level (E_g) in Fig. 3. Apart from E_g, Fig. 3 also depicts the variation with respect to disorder of (i) the SC phase stiffness (ρ_s) and (ii) the average magnetic polarization (m). Based on these indicators, we demarcate the phase diagram into three different phases as (a) gapped (uniform) SC ($E_g \neq 0$, $\rho_s \neq 0$, $m = 0$), (b) gapless SC ($E_g = 0$, $\rho_s \neq 0$, $m \neq 0$), and (c) inhomogeneous polarized Fermi liquid ($E_g = 0$, $\rho_s = 0$, $m \neq 0$). In other words, as a function of increasing disorder strength, we find that the uniform SC gives way to a gapless SC phase at $V_{c1} \sim 0.75$, where the E_g collapses to zero. However, this phase still supports a nonzero value for the global phase stiffness $\rho_s \neq 0$. This implies that quasi-long-range SC phase correlations continue to survive in the gapless regime and vanish only when ρ_s drops to zero at $V_{c2} \sim 1.25$, marking the loss of global SC order. Furthermore, a fit of the magnetic polarization (shown in Fig. 3) to a power-law form $m \sim (V - V_{c1})^{\beta}$ gives $V_{c1} \sim 0.75$ (in consonance with the value one obtains from the closing of the SC gap) and a $\beta \sim 1.5$. The fact that the magnetic polarization picks up as a power law as we enter the gapless phase suggests that it can be used as an order parameter to describe the transition into the gapless phase from the fully gapped superconductor. However, one should note that this continuous transition is a Lifshitz transition and no spontaneous symmetry is broken across it. The spin-dependent asymmetry seen in Fig. 2 for the spin-resolved DOS for $V \geqslant V_{c1} \sim 0.75t$ is another indicator of the system going into a magnetic polarized state. Finally, with increasing disorder strength, the gapless phase gives way to an inhomogeneous polarized Fermi liquid phase.

Now, to get a handle on the physical description of the phases, we study its real-space characterization. More specifically, in Fig. 4 for a single MC snapshot corresponding to a particular disorder realization, we present real-space maps of the (a) pairing field amplitude ($|\Delta_i|$), (b) pairing field phase correlation [$\cos(\theta_0 - \theta_i)$], and (c) magnetic polarization (m_i). In the regime $V < V_{c1}$ as shown in Fig. 4, in real space the state is characterized by a (quasi)-long-ranged, phase correlated, uniform SC state and negligible magnetic polarization. For $V_{c1} < V < V_{c2}$, both the magnetic polarization and pairing field are finite. However, the magnetic polarization in this regime emerges as isolated spatial islands which grow in size with increasing disorder strength. These regions of large magnetic polarization are almost complementary to those of suppressed superconductivity, demonstrating the physics of competing orders where the suppression of one of the order parameters promote the emergence of the other. The physical picture of the phase that one obtains in the regime $V_{c1} < V < V_{c2}$ is that of SC regions where the gap has vanished but still supports a finite phase stiffness, immersed in a matrix of spin-polarized Fermi liquid. The phase stiffness on these isolated SC regions are correlated with respect to each other. Now, as the disorder is increased beyond $V > V_{c2}$, the phase correlation between the islands is lost and we obtain the polarized Fermi liquid with a large magnetic polarization. In other words, this phase is characterized by the survival of short range pair correlations, in the form of phase uncorrelated Josephson junctions. At still stronger disorders (not shown in the figure), the energy states undergo localization [47].

The ground state obtained for the intermediate range of disorder $V_{c1} < V < V_{c2}$ that hosts the two gapless Fermi surfaces with a net magnetic polarization m and a nonvanishing SC phase stiffness ρ_s is the one we identify with the BP or the Liu-Wilczek-Sarma phase.

The origin of this phase can be understood as follows: At the level of the Hamiltonian, the spin-selective disorder potential can be recast as an anticorrelated combination comprising a chemical potential disorder and a random Zeeman field. Thus, spin-dependent disorder maps the model into an imbalanced fermion system with unequal number densities and an asymmetric bandwidth, a disordered version of the Hamiltonian studied in Ref. [48]. The resulting Pauli paramagnetic pair breaking [49,50] arising out of the random Zeeman field generates unpaired fermions which get accommodated as low energy excitation in the gapless BP phase. These unpaired fermions give rise to a nonzero average magnetic polarization in the BP regime, which serves as an order parameter for the phase transition from the gapped SC to the gapless BP phase. In light of the interpretation of the spin-selective disorder into anticorrelated chemical potential disorder and random Zeeman field, it would be tempting to identify the BP elucidated above as a disordered FFLO phase [51]. However, such an identification would be incorrect, as the disordered FFLO state has a nonzero finite momentum pairing, whereas the BP phase discussed here is fundamentally different as the pairing is a zero-momentum pairing. The rewriting of the disorder term in terms of the Zeeman field also allows

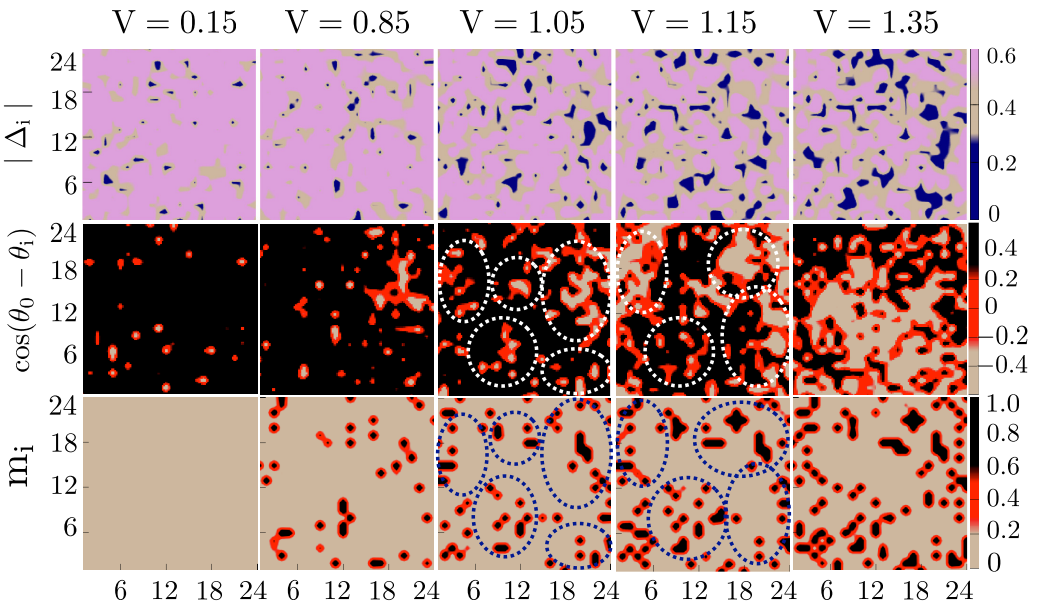

FIG. 4. Spatial evolution of breached pair state with increasing disorder strength. Each column comprises the superconducting pairing field amplitude (| Δ_i |), phase correlation [$\cos(\theta_0 - \theta_i)$] between the phases at a reference site θ_0, and any other site θ_i on the lattice, and magnetic polarization (m_i). Superconducting order and magnetic polarization are weakly complementary, such that the spatial suppression of one promotes the emergence of the other. To highlight this feature, we have used the same color scheme both for the superconducting phase coherence and the magnetic polarization. The circles highlight the representative regions where the maxima in the superconducting phase coherence corresponds to the minima in the magnetic polarization and vice versa.

us to understand the dependence of both V_{c1} and V_{c2} on $|U|$: An increasing $|U|$ implies a concomitant increase in V for the pair breaking to be effective, which in turn implies an increase in the value of V_{c1}. In a similar vein, an increase in U in turn also implies a further increase in value of V_{c2}.

B. The phase diagram as a function of the interaction strength

We next characterize the model by studying its behavior as a function of the interaction strength at a fixed value of disorder which we choose without loss of generality to be $V = 1.05$. In particular, in Fig. 5(a), we plot the SC phase stiffness (ρ_s) and average magnetic polarization (m), as a function of the interaction $| U |$ at a fixed value of the disorder strength $V = 1.05$. Figure 5(a) should be read in conjunction with Fig. 5(b), which shows the behavior of

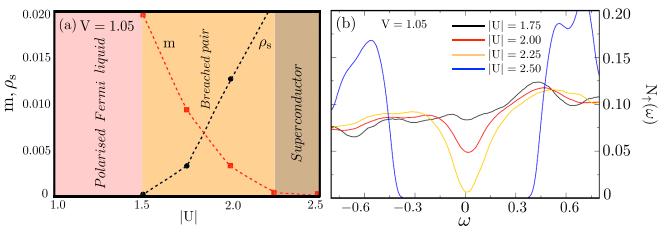

FIG. 5. (a) Ground-state phase diagram at a fixed disorder strength of $V = 1.05$, characterized based on the (i) average magnetic polarization (m) and (ii) superconducting phase stiffness (ρ_s), as a function of interaction strength. (b) The spin-resolved single-particle density of states [$N_\uparrow(\omega)$] at $V = 1.05$ and different interactions $|U|$, demonstrating the evolution from BP to gapped SC phase.

the DOS $N_\uparrow(\omega)$ as a function of energy ω for the selected value of disorder strength and a range of interactions. For the prototypical case in the low interaction regime $|U| = 1.75$, the system supports a finite DOS at the Fermi level consistent with what one expects for a Fermi-liquid state. As we tune up the strength of the interactions, beyond a critical value U_{c1} we enter the BP phase where both ρ_s and m are finite [see Fig. 5(a)]. Concomitantly, as seen in Fig. 5(b), the DOS $N_\uparrow(\omega)$ in this range exhibit signatures of preformed SC pair. Progressive increase in interaction enhances the phase coherence between local SC islands as suggested by the increasingly prominent coherence peaks in the DOS. Note that the asymmetry in the coherence peaks bear out the signature of particle-hole anisotropy. Further increase in interaction beyond a critical value U_{c2} opens a hard gap at the Fermi level (corresponding to an uniform superconductor) while simultaneously suppressing the magnetic polarization to zero. The recasting of the spin-selective disorder into a random chemical potential and a random Zeeman field (both anticorrelated with respect to each other) also allows us to understand the effect of disorder on the values of U_{c1} and U_{c2}: If the disorder strength increases, one needs to go to a larger value of U to set up phase coherence between the SC islands. This implies an increase in U_{c1}. Furthermore, the spin-selective disorder results in a Zeeman gap between the up and down spins which gets enhanced with increasing V. To create a uniform SC state, one has to overcome this Zeeman gap. Thus, for larger values of V, this implies that the value of U_{c2} also increases, (see Fig. 1). Thus, a larger disorder strength requires a stronger interaction strength for the realization of a uniform SC state.

IV. DISCUSSION AND CONCLUSIONS

Through extensive numerical investigations based on the SPA [15,37,44], we have managed to distill the ground-state phase diagram of the attractive Hubbard model in the presence of spin-selective disorder. In particular, we have shown that, apart from the polarized Fermi liquid and the fully gapped superconductor, a gapless BP phase constitutes a stable low-temperature phase in this model.

As evidenced in the real-space maps Fig. 4, to accommodate such a gapless phase, the system breaks up into SC islands where the local gap vanishes, immersed in a sea of polarized fermionic liquid. These gapless superconducting structures still host a fluctuating phase that are correlated over the many superconducting islands such that it supports a nonzero global phase stiffness. This thus alludes to the possibility that the interplay of phase and disorder fluctuations conspire to stabilize a BP-like ground state wherein a net magnetic polarization coexists with gapless superconductivity. The behavior of the DOS at weaker interaction strength can be explained via an adaptation of the AG theory [43,46]. However, a stronger interaction strength requires the development of an effective field theory for the problem at hand, something we leave as a future exercise.

At this juncture, we emphasize that unlike in earlier studies on cold-atomic Fermi-superfluids wherein one had to invoke a momentum-dependent interaction [20–22] to stabilize the so-called Sarma-Liu-Wilczek phase as the ground state, here the BP-type ground state is obtained for a simple Hubbard-like on-site attractive interaction. In fact, using a similar SPA analysis, it was shown conclusively [15] that the BP-type ground state cannot exist as the ground state of a Hubbard model with momentum-independent attractive interaction (on site) in the presence of a Zeeman-field. Furthermore, the FFLO phase that exists at large values of the Zeeman field in the translationally invariant [16] version of the imbalanced Fermi superfluids could be highly susceptible to the effect of disorder (discussed in detail in the next paragraph).

This interplay between disorder and finite magnetic field discussed above raises an interesting question on what are the ground states of an attractive (disordered) Hubbard model wherein the randomness couples directly (at a bare level) to the Zeeman field. In such a scenario of purely random Zeeman field, one expects physics that is very much akin to that of paramagnetic impurities to play out. In other words, the term corresponding to the disordered Zeeman field will look structurally similar to that of paramagnetic impurities in a host superconductor. This would then imply that as the strength of disorder is increased, one expects a transition from a fully gapped BCS-type superconductor to a gapless phase, and finally to a normal state. Now, the question is whether one can stabilize a BP phase by using a purely random Zeeman field. Obviously, just like in this paper, at half filling one cannot obtain a BP phase as the ground state. Away from half filling with purely random Zeeman field, just like the case of the translationally invariant attractive Hubbard model (with point-contact interaction and finite uniform Zeeman field), discussed in the preceding paragraph [15], we believe that the energetics are such that the BP phase cannot be stabilized as the ground state. In other words, in such a scenario with a purely random Zeeman field, at zero temperature, just like in the case of half filling, one expects a direct transition from a gapless phase to a polarized Fermi liquid.

There are several interesting questions that still need to be probed in the context of such a spin-selectively disordered attractive Hubbard model: For instance, even though the Aizenmann-Wehr theorem [52,53] guarantees that the transition from the fully gapped phase to the gapless phase is continuous, the universality class of such a transition remains an open question. One suspects that such a transition may lie in the disordered XY universality class. However, a complete analytical theory attesting to the same is currently lacking. Another important question that remains unanswered in the present paper is the role played by thermal fluctuations in modifying the ground-state phase diagram. We leave the resolution of this relevant issue to a future publication [54]. Another question that is worth pursuing is whether the disorder-induced imbalanced Fermi systems studied here support a non-Fermi liquid phase analogous to the one studied in Ref. [48]. Also, the question on the phase diagram of such a spin-selectively disordered attractive Hubbard model in three dimensions is a very relevant open problem to pursue.

Within the genre of problems discussed above, another interesting problem, especially in the context of cold atoms, would be to study the role of spin-selective disorder on finite-q pairing states such as the FFLO state [7,8]. It is very much plausible that a concomitant scenario to the one discussed in Refs. [51,55,56] arises and, at zero temperature, a disordered FFLO phase obtains even in the presence of spin-selective randomness, intervening between a SC and normal phase. This disordered FFLO phase survives up to a moderate disorder strength, beyond which one obtains a direct transition from the superconductor to the insulator. However, an equally likely scenario would be that the presence of a spin-dependent randomness would melt the FFLO phase (especially in low dimensions) for even infinitesimally small disorder strengths via an Imry-Ma type mechanism [57,58]. Which of these scenarios actually holds true is we believe an open question worth investigating.

Finally, experiments probing the 2D electron gas at the oxide interface (such as $LaAlO_3/SrTiO_3$ heterostructure) have confirmed inhomogeneous spatial coexistence of SC and ferromagnetic correlations [33,59]. Such spatial coexistence gives rise to local magnetic polarization that can be thought to arise due to local Zeeman fields. Now, it is plausible that interplay of such local Zeeman fields with a random chemical potential (stemming from non-magnetic impurities) might lead to spin-selective disorder potential that in turn stabilizes the BP phase.

ACKNOWLEDGMENTS

The authors acknowledge the use of high performance computing cluster Virgo, at IIT, Madras, India. M.K. and R.N. acknowledge funding from the Center for Quantum Information Theory in Matter and Spacetime, IIT Madras. Further, R.N. acknowledges funding from the Department of Science and Technology, Govt. of India, under Grant No. DST/ICPS/QuST/Theme-3/2019/Q69. The authors are

also very grateful to Shashikant Singh Kunwar, Prabuddha Chakraborty, Igor Gornyi, Igor Burmistrov, and G. Baskaran for discussions on this and related works.

APPENDIX

1. Static path approximation *vis a vis* other techniques

In this Appendix, we briefly elucidate the approximation that is entailed in the SPA method and compare it with other well-known methods that are currently in vogue.

To start, we express the partition function of the Hubbard model in terms of a functional integral over Grassmann valued fields $\psi_{i\sigma}(\tau)$, $\bar{\psi}_{i\sigma}(\tau)$ as

$$Z = \int \mathcal{D}\psi \mathcal{D}\bar{\psi} e^{-S[\psi,\bar{\psi}]},$$

$$S = \int_0^\beta d\tau \Bigg[\sum_{ij,\sigma} \{\bar{\psi}_{i\sigma}((\partial_\tau - \mu)\delta_{ij} - t_{ij})\psi_{j\sigma}\} + |U| \sum_{i,\sigma,\sigma'} \bar{\psi}_{i\sigma}\psi_{i\sigma}\bar{\psi}_{i\sigma'}\psi_{i\sigma'} \Bigg]. \quad \text{(A1)}$$

Since only quadratic path integrals can be exactly evaluated, the presence of a quartic interaction term in the partition function poses an immediate problem that it cannot be evaluated exactly.

To make progress, following Refs. [16,37,44], we take recourse to the HS transformation to decouple the quartic term. In other words, we rewrite the partition function in terms of the pairing field $\Delta_i(\tau)$, $\bar{\Delta}_i(\tau)$ and charge field $\phi_i(\tau)$. Written in terms of the HS fields, the partition function Eq. (A1) can be recast as

$$Z = \int \mathcal{D}\Delta\mathcal{D}\Delta^*\mathcal{D}\phi\mathcal{D}\psi\mathcal{D}\bar{\psi} e^{-S_1[\psi,\bar{\psi},\phi,\Delta,\Delta^*]},$$

$$S_1 = \int_0^\beta d\tau \Bigg[\sum_{ij,\sigma} \{\bar{\psi}_{i\sigma}((\partial_\tau - \mu)\delta_{ij} - t_{ij})\psi_{j\sigma}\} - \sum_i \left\{ \Delta_i(\tau)\bar{\psi}_{i\uparrow}(\tau)\bar{\psi}_{i\downarrow}(\tau) + \text{H.c.} - \frac{|\Delta_i|^2}{|U|} \right\} + \sum_i \{i\phi_i \sum_{\sigma,\sigma'} \bar{\psi}_{i\sigma}(\tau)\psi_{i\sigma'}(\tau)\delta_{\sigma\sigma'} + \frac{\phi_i^2}{|U|}\} \Bigg]. \quad \text{(A2)}$$

The integral over the Grassmanian fields $(\psi, \bar{\psi})$ are now purely quadratic, however, we pay a cost in terms of the extra integrations over the HS fields $\Delta_i(\tau)$, $\Delta_i^*(\tau)$, and $\phi_i(\tau)$. Note that at this point, Eq. (A3) is an exact rewriting of the Hubbard model of Eq. (A1).

The quadratic integration over the Grassmanian fields can be formally carried out, thus providing the weight factor for the Δ_i and ϕ_i configurations. Thus,

$$Z = \int \mathcal{D}\phi\mathcal{D}\Delta\mathcal{D}\Delta^* e^{-S_2[\Delta,\Delta^*,\phi]},$$

$$S_2 = \log \text{Det}[\mathcal{G}^{-1}\{\Delta,\phi\}] + \frac{|\Delta_i|^2}{|U|} + \frac{\phi_i^2}{|U|}. \quad \text{(A3)}$$

Here, in Eq. (A3), $\mathcal{G}$ is the electron Green's function in a $\{\Delta_i, \phi_i\}$ background.

Furthermore, it is obvious from Eq. (A3) that the weight factor for an arbitrary space-time configuration $\{\Delta_i(\tau), \phi_i(\tau)\}$ involves computation of the fermionic determinant in that background. Now, we invoke the SPA [15,44], which involves dropping the imaginary time (τ) dependence of the auxiliary or HS fields. In other words, at this juncture we only retain the $\Omega_n = 0$ Matsubara frequency mode. However, the model retains within itself spatial fluctuations at all scales.

For further clarity, we now compare the SPA scheme we utilize to other well-known techniques:

(1) The quantum MC retains the full i, Ω_n dependence of the HS fields Δ and ϕ computing $\log \text{Det}[\mathcal{G}^{-1}\{\Delta,\phi\}]$ iteratively for importance sampling. The approach is valid at all T, but to obtain the real frequency spectra, one needs to do a computationally difficult analytic continuation.

(2) MFT essentially implies that the HS fields $\Delta_i(\Omega_n)$ and $\phi_i(\Omega_n)$ are spatially uniform (or periodic) and time independent ($\Omega_n = 0$) modes, i.e., $\Delta_i(\Omega_n) \to \Delta$ and $\phi_i(\Omega_n) \to \phi$.

(3) DMFT: The DMFT treatment has the full dynamics of the problem, however, the HS fields Δ and ϕ are evaluated at effectively a single site, i.e., $\Delta_i(\Omega_n) \to \Delta(\Omega_n)$ and $\phi_i(\Omega_n) \to \phi(\Omega_n)$. This is an exact treatment when dimensionality $D \to \infty$.

2. Details of the Monte Carlo method

Here, we briefly discuss some of the more salient points related to the MC method that we employ to study the spin-selectively disordered superconductor. We use the traveling cluster approximation (TCA), (see Ref. [15] for more details). Within this scheme, instead of diagonalizing the full $N = L \times L$ lattice Hamiltonian for each attempted update of the auxiliary fields $\{\Delta_i, \phi_i\}$, a smaller cluster (of size $N_c = L_c \times L_c$) surrounding the update site is diagonalized. Thus, employing this TCA, the cost of diagonalization of the matrix is brought down from $\sim O(N^4)$, per lattice sweep to $\sim N O(N_c^3)$. This linear scaling in N that stems from using the TCA allows us to access lattice sizes up to $\sim 40 \times 40$, whereas standard routines based on the diagonalization of the full lattice Hamiltonian for each attempted MC update would restrict us to system size to $\sim 12 \times 12$ (for a reasonable computation cost) even with the SPA. In our calculations, we have used a cluster dimension $L_c = 6$, (going to larger cluster sizes does not change our results).

In what follows, we briefly discuss the details of our MC calculations. Our calculations are carried out over 4000 MC sweeps. Out of these, we equilibrate over the first 2000 sweeps. Out of the remaining 2000 sweeps, 200 configurations are saved over which the correlation functions were computed. Increasing the number of MC sweeps any further does not alter the results presented in this paper. In a similar vein, we have verified that increasing the number of disorder realization (up to 20) does not affect our results.

3. Bogoliubov–de Gennes formalism

In this section, we compare the results obtained from a self-consistent (inhomogeneous) BdG MFT applied to

the s-wave superconductor with spin-selective potential disorder [42,43] to those obtained from the SPA analysis obtained in the main part of this paper. Within the BdG scheme, the s-wave singlet pairing is defined as $\Delta_i = U\langle c_{i\downarrow} c_{i\uparrow}\rangle$ while the charge order parameter is defined as $\phi_i = \frac{U}{2}(n_{i\uparrow} + n_{i\downarrow}) = \frac{U}{2}(\langle c^\dagger_{i\uparrow} c_{i\uparrow}\rangle + \langle c^\dagger_{i\downarrow} c_{i\downarrow}\rangle)$, where U is the on-site interaction. We diagonalize the effective Hamiltonian by using the Bogoliubov-Valatin transformations, $c_{i,\sigma} = \sum_m (u_{m,i\sigma}\gamma_{m,\sigma} - s_\sigma v^*_{m,i\sigma}\gamma^\dagger_{m-\sigma})$, where $\gamma^\dagger_{m\sigma}(\gamma_{m\sigma})$ correspond to the creation (annihilation) operators of the Bogoliubov quasiparticles with spin σ and energy ϵ^σ_m and wave functions $u_{mi\sigma}$ and $v_{mi\sigma}$. We have introduced spin index $s_\uparrow = 1$ and $s_\downarrow = -1$. The resulting gap and number equations are

$$\Delta_i = U\sum_m \{v^*_{mi\downarrow} u_{mi\uparrow} f(\epsilon_{m\uparrow}) + u^*_{mi\downarrow} v_{mi\uparrow} f(\epsilon_{m\downarrow})\},$$
$$n_i = \sum_m \{|\, u_{mi\uparrow}\,|^2 f(\epsilon_{m\uparrow}) + |\, v_{mi\uparrow}\,|^2 f(\epsilon_{m\downarrow})\} + \sum_m \{|\, u_{mi\downarrow}\,|^2 [1 - f(\epsilon_{m\uparrow})] + |\, v_{mi\downarrow}\,|^2 [1 - f(\epsilon_{m\downarrow})]\}, \tag{A4}$$

where $f(\epsilon_m)$ is the Fermi function. For each disorder realization starting from an initial guess value, these equations are iteratively solved till self consistent values are obtained for Δ_i and ϕ_i. The thermodynamic indicators such as the magnetic polarization m and the pairing field structure factor $S(\mathbf{q}) = (1/N)\sum_{ij} \Delta^*_i \Delta_j e^{i\mathbf{q}.(\mathbf{r}_i - \mathbf{r}_j)}$ are obtained after averaging over the disorder realizations (we average over 20 different disorder realizations to compute our thermodynamic quantities). The resulting ground state (as obtained from the converged solutions) is finally characterized based on these disorder averaged thermodynamic indicators m and $S(\mathbf{q})$.

Figure 6 shows the magnetic polarization and structure factor obtained using the BdG formalism, in comparison to those obtained via the SPA technique. From Fig. 6, we see that there are some salient differences between the results garnered by using the SPA formalism as opposed to those obtained by using the BdG method: From Fig. 6, it is obvious that the value of V_{c2} [where $m \neq 0$ and $S(\mathbf{q}) = 0$] as calculated from SPA is at $V_{c2} = 1.25$, whereas the $S(\mathbf{q})$ evaluated by using the BdG method is still finite and vanishes for much larger V. Furthermore, as is clear from Fig. 6, the disorder dependence of the pairing field correlation $[S(\mathbf{q})]$ as obtained by the two approaches behave differently. These discrepancies stem from the fact that unlike the BdG treatment, SPA incorporates phase fluctuations that lead to rapid suppression of the pairing field correlations as suggested by the exponential decay of $S(\mathbf{q})$ at large V.

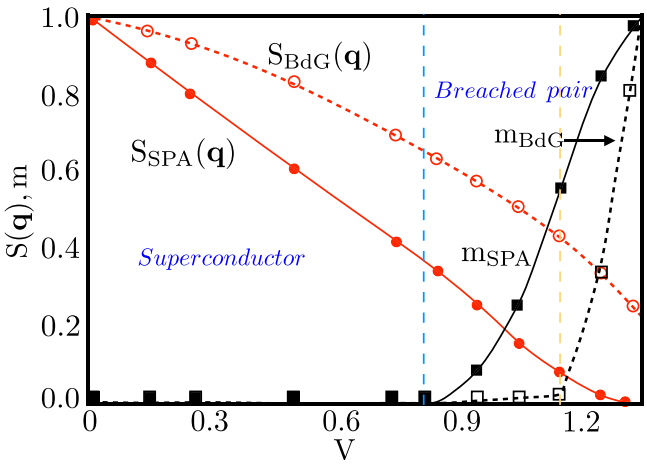

FIG. 6. Disorder dependence of superconducting pairing field structure factor $[S(\mathbf{q})]$ and average polarization $\langle m_i\rangle$ as obtained using BdG mean field (dashed curves) and SPA (solid curves) approaches. The blue dashed line indicates the phase transition (of the Lifshitz type) between the uniform superconductor and breached-pair phase, as determined using SPA, while the orange dashed line corresponds to the same as determined using BdG. The calculations are carried out at $n \sim 0.85$, $|\, U\,| = 2$, $T = 0.01$, and for a system size of $L = 32$.

[1] G. Simon, M. Bartkowiak, J. Gavilano, E. Ressoiche, N. Egetenmeyer, C. Niedermayer, A. D. Bianchi, R. Movshovich, E. D. Bauer, J. D. Thompson, and M. Kenzelmann, Switching of magnetic domains reveals spatially inhomogeneous superconductivity, Nat. Phys. **10**, 126 (2013).

[2] H. Mayaffre, S. Kramer, M. Horvati, C. Berthier, K. Miyagawa, K. Kanoda, and V. F. Mitrovic, Evidence of Andreev bound states as a hallmark of the FFLO phase in κ-(BEDT-TTF)$_2$ Cu(NCS)$_2$, Nat. Phys. **10**, 928 (2014).

[3] D. A. Zocco, K. Grube, F. Eilers, T. Wolf, and H. v. Löhneysen, Pauli-Limited Multiband Superconductivity in KFe_2 As_2, Phys. Rev. Lett. **111**, 057007 (2013).

[4] Y.-A. Liao, A. Sophie C. Rittner, T. Paprotta, W. Li, G. B. Partridge, R. G. Hulet, S. K. Baur, and E. J. Mueller, Spin-imbalance in a one-dimensional Fermi gas, Nature (London) **467**, 567 (2010).

[5] Y-I. Shin, C. H. Schunck, A. Schirotzek, and W. Ketterle, Phase diagram of a two-component Fermi gas with resonant interactions, Nature (London) **451**, 689 (2008).

[6] G. B. Partridge, W. Li, Y. A. Liao, R. G. Hulet, M. Haque, and H. T. C. Stoof, Deformation of a Trapped Fermi Gas with Unequal Spin Populations, Phys. Rev. Lett. **97**, 190407 (2006).

[7] P. Fulde and R. A. Ferrell, Superconductivity in a strong spin-exchange field, Phys. Rev. **135**, A550 (1964).

[8] A. I. Larkin and Y. N. Ovchinnikov, Nonuniform state of superconductors, Zh. Eksp. Teor. Fiz. **47**, 1136 (1964).

[9] Y. Lee Loh and N. Trivedi, Detecting the Elusive Larkin-Ovchinnikov Modulated Superfluid Phases for Imbalanced Fermi Gases in Optical Lattices, Phys. Rev. Lett. **104**, 165302 (2010).

[10] T. K. Koponen, T. Paananen, J.-P. Martikainen, and P. Törmä, Finite-Temperature Phase Diagram of a Polarized Fermi Gas in an Optical Lattice, Phys. Rev. Lett. **99**, 120403 (2007).

[11] M. J. Wolak, B. Grémaud, R. T. Scalettar, and G. G. Batrouni, Pairing in a two-dimensional Fermi gas with population imbalance, Phys. Rev. A **86**, 023630 (2012).

[12] S. Chiesa and S. Zhang, Phases of attractive spin-imbalanced fermions in square lattices, Phys. Rev. A **88**, 043624 (2013).
[13] M. O. J. Heikkinen, D.-H. Kim, and P. Torma, Finite-temperature stability and dimensional crossover of exotic superfluidity in lattices, Phys. Rev. B **87**, 224513 (2013).
[14] M. O. J. Heikkinen, D.-H. Kim, M. Troyer, and P. Torma, Nonlocal Quantum Fluctuations and Fermionic Superfluidity in the Imbalanced Attractive Hubbard Model, Phys. Rev. Lett. **113**, 185301 (2014).
[15] M. Karmakar and P. Majumdar, Population-imbalanced lattice fermions near the BCS-BEC crossover: Thermal physics of the breached pair and fulde-ferrell-larkin-ovchinnikov phases, Phys. Rev. A **93**, 053609 (2016).
[16] M. Karmakar, Thermal transitions, pseudogap behavior, and BCS-BEC crossover in Fermi-Fermi mixtures, Phys. Rev. A **97**, 033617 (2018).
[17] G. Sarma, On the influence of a uniform exchange field acting on the spins of the conduction electrons in a superconductor, J. Phys. Chem. Solids **24**, 1029 (1963).
[18] W. V. Liu and F. Wilczek, Interior Gap Superfluidity, Phys. Rev. Lett. **90**, 047002 (2003).
[19] P. F. Bedaque, H. Caldas, and G. Rupak, Phase Separation in Asymmetrical Fermion Superfluids, Phys. Rev. Lett. **91**, 247002 (2003).
[20] M. McNeil Forbes, E. Gubankova, W. V. Liu, and F. Wilczek, Stability Criteria for Breached-Pair Superfluidity, Phys. Rev. Lett. **94**, 017001 (2005).
[21] K. Yang and S. L. Sondhi, Response of a $d_{x^2-y^2}$ superconductor to a zeeman magnetic field, Phys. Rev. B **57**, 8566 (1998).
[22] M. Karmakar, Pauli limited *d*-wave superconductors: Quantum breached pair phase and thermal transitions, J. Phys.: Condens. Matter **32**, 405604 (2020).
[23] D. Y. Kim, S.-Z. Lin, F. Weickert, M. Kenzelmann, E. D. Bauer, F. Ronning, J. D. Thompson, and R. Movshovich, Intertwined Orders in Heavy-Fermion Superconductor $CeCoIn_5$, Phys. Rev. X **6**, 041059 (2016).
[24] S.-Zeng Lin, D. Y. Kim, E. D. Bauer, F. Ronning, J. D. Thompson, and R. Movshovich, Interplay of the Spin Density Wave and a Possible Fulde-Ferrell-Larkin-Ovchinnikov State in $CeCoIn_5$ in Rotating Magnetic Field, Phys. Rev. Lett. **124**, 217001 (2020).
[25] D. McKay and B. DeMarco, Thermometry with spin-dependent lattices, New J. Phys. **12**, 055013 (2010).
[26] O. Mandel, M. Greiner, A. Widera, T. Rom, T. W. Hansch, and I. Bloch, Controlled collisions for multi-particle entanglement of optically trapped atoms, Nature (London) **425**, 937 (2003).
[27] A. E. Feiguin and M. P. A. Fisher, Exotic Paired States with Anisotropic Spin-Dependent Fermi Surfaces, Phys. Rev. Lett. **103**, 025303 (2009).
[28] W. V. Liu, F. Wilczek, and P. Zoller, Spin-dependent Hubbard model and a quantum phase transition in cold atoms, Phys. Rev. A **70**, 033603 (2004).
[29] O. Mandel, M. Greiner, A. Widera, T. Rom, T. W. Hänsch, and I. Bloch, Coherent Transport of Neutral Atoms in Spin-Dependent Optical Lattice Potentials, Phys. Rev. Lett. **91**, 010407 (2003).
[30] A. Ohtomo and H. Y. Hwang, A high-mobility electron gas at the $LaAlO_3/SrTiO_3$ heterointerface, Nature (London) **427**, 423 (2004).
[31] M. Zhang, K. Du, T. Ren, H. Tian, Z. Zhang, H. Y. Hwang, and Y. Xie, A termination-insensitive and robust electron gas at the heterointerface of two complex oxides, Nat. Commun. **10**, 4026 (2019).
[32] K. Han, K. Hu, X. Li, K. Huang, Z. Huang, S. Zeng, D. Qi, C. Ye, J. Yang, H. Xu, A. Ariando, J. Yi, W. Lae, S. Yan, and X. R. Wang, Erasable and recreatable two-dimensional electron gas at the heterointerface of $SrTiO_3$ and a water-dissolvable overlayer, Sci. Adv. **5**, eaaw7286 (2019).
[33] F. Bi, M. Huang, S. Ryu, H. Lee, C.-W. Bark, C.-B. Eom, P. Irvin, and J. Levy, Room-temperature electronically-controlled ferromagnetism at the $LaAlO_3/SrTiO_3$ interface, Nat. Commun. **5**, 5019 (2014).
[34] V. J. Emery, Theory of the quasi-one-dimensional electron gas with strong "on-site" interactions, Phys. Rev. B **14**, 2989 (1976).
[35] R. T. Scalettar, E. Y. Loh, J. E. Gubernatis, A. Moreo, S. R. White, D. J. Scalapino, R. L. Sugar, and E. Dagotto, Phase Diagram of the Two-Dimensional Negative-*U* Hubbard Model, Phys. Rev. Lett. **62**, 1407 (1989).
[36] A. Ghosal, M. Randeria, and N. Trivedi, Inhomogeneous pairing in highly disordered s-wave superconductors, Phys. Rev. B **65**, 014501 (2001).
[37] Y. Dubi, Y. Meir, and Y. Avishai, Nature of the superconductor-insulator transition in disordered superconductors, Nature (London) **449**, 876 (2007).
[38] S. Tarat and P. Majumdar, Charge dynamics across the disorder-driven superconductor-insulator transition, Europhys. Lett. **105**, 67002 (2014).
[39] K. Bouadim, Y. Lee Loh, M. Randeria, and N. Trivedi, Single-and two-particle energy gaps across the disorder-driven superconductor-insulator transition, Nat. Phys. **7**, 884 (2011).
[40] M. Swanson, Y. Lee Loh, M. Randeria, and N. Trivedi, Dynamical Conductivity Across the Disorder-Tuned Superconductor-Insulator Transition, Phys. Rev. X **4**, 021007 (2014).
[41] Y. Lee Loh, M. Randeria, N. Trivedi, C.-C. Chang, and R. Scalettar, Superconductor-Insulator Transition and Fermi-Bose Crossovers, Phys. Rev. X **6**, 021029 (2016).
[42] M. Jiang, R. Nanguneri, N. Trivedi, G. G. Batrouni, and R. T. Scalettar, Gapless inhomogeneous superfluid phase with spin-dependent disorder, New J. Phys. **15**, 023023 (2013).
[43] R. Nanguneri, M. Jiang, T. Cary, G. G. Batrouni, and R. T. Scalettar, Interplay of superconductivity and spin-dependent disorder, Phys. Rev. B **85**, 134506 (2012).
[44] W. E. Evenson, J. R. Schrieffer, and S. Q. Wang, New approach to the theory of itinerant electron ferromagnets with local-moment characteristics, J. Appl. Phys. **41**, 1199 (1970).
[45] G. Seibold, L. Benfatto, C. Castellani, and J. Lorenzana, Superfluid Density and Phase Relaxation in Superconductors with Strong Disorder, Phys. Rev. Lett. **108**, 207004 (2012).
[46] A. A. Abrikosov and L. P. Gor'kov, Contribution to the theory of superconducting alloys with paramagnetic impurities, JETP **12**, 1243 (1961).
[47] In two dimensions, according to Anderson's theorem, all states would be localized. However, for moderate disorder the localization length would be large compared to the system sizes. Thus, the polarized Fermi liquid is most probably a finite-size

artifact and will become an insulator in the true thermodynamic limit.

[48] P. Strack and P. Jakubczyk, Fluctuations of Imbalanced Fermionic Superfluids in Two Dimensions Induce Continuous Quantum Phase Transitions and Non-Fermi-Liquid Behavior, Phys. Rev. X **4**, 021012 (2014).

[49] A. M. Clogston, Upper Limit for the Critical Field in Hard Superconductors, Phys. Rev. Lett. **9**, 266 (1962).

[50] B. S. Chandrasekhar, A note on the maximum critical field of high-field superconductors, Appl. Phys. Lett. **1**, 7 (1962).

[51] Q. Cui and K. Yang, Fulde-Ferrell-Larkin-Ovchinnikov state in disordered *s*-wave superconductors, Phys. Rev. B **78**, 054501 (2008).

[52] M. Aizenman and J. Wehr, Rounding of First-Order Phase Transitions in Systems with Quenched Disorder, Phys. Rev. Lett. **62**, 2503 (1989).

[53] K. Hui and A. N. Berker, Random-Field Mechanism in Random-Bond Multicritical Systems, Phys. Rev. Lett. **62**, 2507 (1989).

[54] M. Karmakar, P. Chakraborty, and R. Narayanan (unpublished).

[55] Y. Yanase, The disordered Fulde-Ferrel-Larkin-Ovchinnikov state in *d*-wave superconductors, New J. Phys. **11**, 055056 (2009).

[56] Y. L. Loh, N. Trivedi, Y. M. Xiong, P. W. Adams, and G. Catelani, Origin of Excess Low-Energy States in a Disordered Superconductor in a Zeeman Field, Phys. Rev. Lett. **107**, 067003 (2011).

[57] S. Singh Kunwar, A. Sen, T. Vojta, and R. Narayanan, Tuning a random-field mechanism in a frustrated magnet, Phys. Rev. B **98**, 024206 (2018).

[58] Y. Imry and S.-k. Ma, Random-Field Instability of the Ordered State of Continuous Symmetry, Phys. Rev. Lett. **35**, 1399 (1975).

[59] J. A. Bert, B. Kalisky, C. Bell, M. Kim, Y. Hikita, H. Y. Hwang, and K. A. Moler, Direct imaging of the coexistence of ferromagnetism and superconductivity at the $LaAlO_3/SrTiO_3$ interface, Nat. Phys. **7**, 767 (2011).